Analysis of the crystallization kinetics in the semiconducting glassy alloy $Cu_{0.20}As_{0.35}Te_{0.45}$

C. Wagner*, J. Vázquez, M. Domínguez, P. Villares, R. Jiménez-Garay

Facultad de Ciencias, Universidad de Cádiz, Apartado 40, Puerto Real (Cádiz), Spain

Abstract

A study of the crystallization kinetics of the glassy alloy $Cu_{0.20}As_{0.35}Te_{0.45}$ was made using a method in which the crystallization rate is deduced bearing in mind the dependence of the reaction rate constant on time, through temperature. The method was applied to the experimental data obtained by differential scanning calorimetry, using continuous heating techniques. The alloy studied exhibited overlapping exothermic peaks, which were resolved using a numerical method developed by the authors, making it possible to study the crystallization phases separately. The kinetic parameters determined for each stage have made it possible to discuss the different types of nucleation and crystal growth exhibited by each stage of the crystallization process. The phases at which the alloy crystallizes after the thermal process have been identified by X-ray diffraction. In both stages of the process, microcrystallites of As_2Te_3 and Cu_7Te_5 are crystallized in an amorphous matrix. In the second stage, a small amount of the crystalline phase CuTe appears, coexisting with the aforementioned crystalline compounds.

Keywords: Crystallization; Nucleation; Reaction rate

1. Introduction

The study of crystallization kinetics in amorphous materials by differential scanning calorimetry (DSC) methods has been discussed in Refs. [1–3]. There is a large variety of theoretical models and theoretical functions proposed to explain the crystallization kinetics. The application of each of them depends on the type of amorphous material studied and how it was made. For chalcogenide glasses obtained in bulk form, which is the case for the alloy $Cu_{0.20}As_{0.35}Te_{0.45}$ we studied [4], the most adequate theoretical model turned out to be the so-called Johnson–Mehl–Avrami (JMA) model, which, although developed for isothermal processes, can be applied under certain conditions to continuous heating experiments [3], thus obtaining satisfactory kinetic parameters (activation energy E, reaction order n, and frequency factor K_0) for describing the crystallization reactions.

The present paper studies the crystallization kinetics of the glassy alloy $Cu_{0.20}As_{0.35}Te_{0.45}$, which is charac-

terized by the aforementioned parameters, using differential scanning calorimetry with continuous-heating techniques. Finally, the crystalline phases corresponding to different stages of the exothermic reactions were identified by X-ray diffraction (XRD) measurements, using Cu Kα radiation.

2. Theoretical analysis

The theoretical basis for the interpretation of the DSC results is provided by the formal theory of transformation kinetics, as developed by Johnson, Mehl and Avrami [5,6]. In its basic form, the theory describes the evolution with time t of the crystallized fraction x in terms of the nucleation frequency per unit volume, I_v, and the crystalline growth rate u:

$$x = 1 - \exp\left[-g \int_0^t I_v \left(\int_{t'}^t u \, d\tau \right)^m dt' \right] \tag{1}$$

where g is a geometric factor which depends on the shape of the crystalline growth and m is a parameter

* Corresponding author.

which depends on the mechanisms of growth and the dimensionality of the crystal. For the important case of isothermal crystallization with time-independent nucleation and growth rates, Eq. (1) can be integrated to obtain

$$x = 1 - \exp(-g'I_v u^m t^n) \qquad (2)$$

where $n = m + 1$ for $I_v \neq 0$ and g' is a new shape factor. Expression (2) can be identified with the Johnson–Mehl–Avrami relationship

$$x = 1 - \exp[-(Kt)^n] \qquad (3)$$

in which K is defined as the reaction rate constant, which is usually assigned an Arrhenian temperature dependence

$$K = K_0 e^{-E/RT} \qquad (4)$$

where E is the effective activation energy which describes the overall crystallization process and K_0 is the frequency factor. Comparison of Eqs. (2) and (3) shows that K^n is proportional to $I_v u^m$, and therefore the consideration of an Arrhenian temperature dependence for K is valid only when I_v and u vary with temperature in an Arrhenian manner.

In general, nucleation frequency and crystalline growth rate exhibit far from Arrhenius-type behaviour [7,8]; however, for a sufficiently limited temperature range, such as the range of crystallization peaks in DSC experiments, both magnitudes can be considered to exhibit the said behaviour.

It is a well-known fact that Eqs. (3) and (4) are used as the basis of nearly all differential thermal analysis (DTA) and DSC crystallization experiments, but it must be noted that expression (3) can be applied accurately only in experiments carried out under isothermal conditions, for which it was deduced. However, this expression is often used for deducing relationships describing non-isothermal crystallization processes, because the values obtained for kinetic parameters are in good agreement with those determined through other methods. From this point of view, the crystallization rate is obtained by deriving expression (3) with respect to time, bearing in mind the fact that, in the non-isothermal process, the reaction rate constant is a time function through its Arrhenian temperature dependence [9], resulting in

$$\frac{dx}{dt} = n(Kt)^{n-1}\left(t\frac{dK}{dt} + K\right)(1 - x) \qquad (5)$$

The maximum crystallization rate is found by making $d^2x/dt^2 = 0$, thus obtaining the relationship

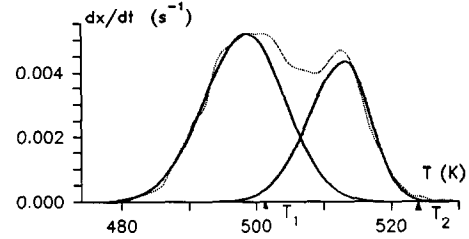$$[n - 1 - n(Kt)^n]\left(t\frac{dK}{dt} + K\right)^2 + Kt\left(2\frac{dK}{dt} + t\frac{d^2K}{dt^2}\right) = 0 \qquad (6)$$

Fig. 1. Resolution of overlapping peaks through the associated theoretical functions representing them for a heating rate of 8 K min^{-1} (associated theoretical functions ——, experimental curve $\cdots$).

in which, by substituting dK/dt and d^2K/dt^2 for their expressions, introducing the heating rate $\beta = dT/dt$ and considering $T = T_0 + \beta t$ (T_0 being the initial temperature), we obtain the expression

$$\left(\frac{K_p(T_p - T_0)}{\beta}\right)^n = 1 - \frac{1}{n}\left[1 + \frac{2E}{RT_p}\left(\frac{T_p - T_0}{T_p}\right)^2\right]$$
$$\times \left(1 + \frac{E}{RT_p^2}(T_p - T_0)\right)^{-2} \qquad (7)$$

which relates the kinetic crystallization parameters E and n to the magnitude values (denoted by subscript p) that can be determined experimentally, and which correspond to the maximum crystallization rate. For most crystallization reactions one typically observes that $[(T_p - T_0)/T_p]^2 \ll 1$, and Eq. (7) becomes

$$\left(\frac{K_p(T_p - T_0)}{\beta}\right)^n = 1 - \frac{1}{n}\left(1 + \frac{E}{RT_p^2}(T_p - T_0)\right)^{-2} \qquad (8)$$

It should be noted that in non-isothermal crystallization experiments where the reaction rate constant may be considered to be temperature dependent, according to the Arrhenius relationship, the activation energy E of the process is much larger than RT_p, in which case it is verified that

$$y_p = \left(\frac{K_p(T_p - T_0)}{\beta}\right)^n \approx 1 \qquad (9)$$

an expression from which it is deduced that the crystallized fraction for the maximum crystallization rate is 0.63, which, as may be observed, is independent of the heating rate and the reaction order. The logarithmic form of Eq. (9) is

$$\ln\frac{T_p - T_0}{\beta} = \frac{E}{R}\frac{1}{T_p} - \ln K_0 \qquad (10)$$

a linear relationship which makes it possible to calculate the parameters E and K_0. At the same time, if the relationship $K_p(T_p - T_0)/\beta = 1$ is introduced into Eq. (5), we obtain

$$n = \frac{dx}{dt}\bigg|_p RT_p^2(0.37EK_p(T_p - T_0))^{-1} \qquad (11)$$

Table 1
Parameters (a, b_1, b_2, T_p) that make it possible to resolve the overlapping peaks of alloy $Cu_{0.20}As_{0.35}Te_{0.45}$ for the different experimental heating rates

β (K min^{-1})	1st stage				2nd stage			
	$10^3 a$ (s^{-1})	$10^2 b_1$ (K^{-2})	$10^2 b_2$ (K^{-2})	T_p (K)	$10^3 a$ (s^{-1})	$10^2 b_1$ (K^{-2})	$10^2 b_2$ (K^{-2})	T_p (K)
2	1.867	3.701	4.154	485.8	0.905	23.416	7.165	497.6
4	3.033	2.858	2.985	489.5	1.757	9.773	9.388	504.0
8	5.193	2.982	3.556	498.6	4.324	4.007	8.690	513.3
16	9.584	2.119	2.041	503.7	8.023	9.844	7.768	519.4
32	14.761	1.164	0.885	511.3	10.19	11.063	4.698	528.2

which makes it possible to calculate the reaction order or kinetic exponent n.

3. Experimental

Bulk $Cu_{0.20}As_{0.35}Te_{0.45}$ glass was prepared by the standard melt quenching method. High purity (99.999%) copper, arsenic and tellurium in appropriate atomic percent proportions were weighed (total 7 g per batch) into quartz glass ampoules. The contents were sealed under a vacuum of 10^{-4} torr, heated to 900 °C for about 5 h and then quenched in ice water, which supplied the necessary cooling rate for obtaining the glass. The ampoules were continuously rotated in the furnace to homogenize the contents. The amorphous nature of the material was checked through a diffractometric X-ray scan, in a Siemens D500 diffractometer. Thermal behaviour was tested using a Thermoflex differential scanning calorimeter by Rigaku. Temperature and energy calibrations of the instrument were performed using the well-known melting temperatures and melting enthalpies of high-purity tin, lead and indium supplied with the instrument. Powdered samples of about 20 mg were crimped (but not sealed) in an aluminum pan and scanned at room temperature through their T_g at heating rates of 2, 4, 8, 16 and 32 K min^{-1}. An empty aluminum pan was used as reference, and in all cases a constant 60 ml min^{-1} flow of He-55 was maintained in order to drag the gases emitted by the reaction, which are highly corrosive to the sensor equipment installed in the DSC furnace. The glass transition temperatures T_g were considered to be the temperature corresponding to the intersection of the two linear portions joining the transition elbow in the DSC trace. The crystallization temperatures T_p were identified as those corresponding to the maximum of each peak. The initial temperatures T_0 of the reactions were identified as the corresponding inflexions in the thermograms.

The DSC register gives two crystallization overlapping peaks for the glassy alloy $Cu_{0.20}As_{0.35}Te_{0.45}$, as shown in Fig. 1. The resolution of overlapping peaks is a question of numerical calculation, which is explained in detail in the literature [10] and used in this work to study the multiphase crystallization exhibited for the alloy studied.

With the aim of investigating the phases at which the samples crystallize, diffractograms of the material crystallized during the DSC were obtained. The experiments were performed with a Philips diffractometer (type PW 1830). The patterns were run with Cu as target and Ni as filter ($\lambda = 1.542$ Å) at 40 kV and 40 mA, with a scanning speed of 0.1 °C s^{-1}.

4. Crystallization kinetics

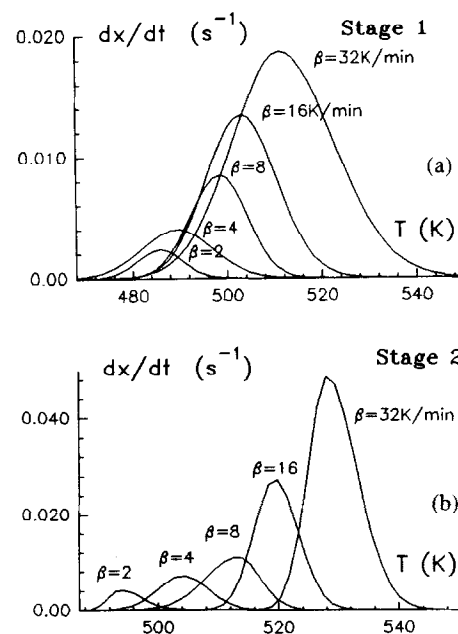The area under the DSC curve is directly proportional to the total amount of alloy crystallized. The

Fig. 2. Crystallization rate vs. temperature, found from the theoretical functions for each stage at different heating rates.

Table 2
Initial peak temperature T_0, maximum peak temperature T_p, and calculated enthalpies, corresponding to the different experimental heating rates

β (K min^{-1})	Peak 1			Peak 2		
	T_0 (K)	T_p (K)	ΔH (mcal mg^{-1})	T_0 (K)	T_p (K)	ΔH (mcal mg^{-1})
2	476.0	485.8	4.49	491.9	497.6	1.21
4	474.2	489.5	4.24	495.8	504.0	1.36
8	486.1	498.6	3.31	502.5	513.3	2.09
16	488.9	503.7	2.60	512.5	519.4	2.90
32	491.3	511.3	3.31	521.7	528.2	0.88

ratio between the ordinates and the total area gives the corresponding crystallization rates, as shown in Fig. 1 (dotted line). The resolution of the overlapping peaks implies, according to the literature [10], calculation of the parameters a, b_1, b_2 and T_p shown in Table 1, for each experimental heating rate. The crystallization kinetics in this case is studied, taking the data derived from the associated theoretical functions as the experimental data. The crystallization rate curves are shown in Fig. 2, and Table 2 gives the characteristic temperatures of all these curves, as well as the enthalpies, for each stage of the process, calculated for different heating rates. It may be observed that the $(dx/dt)_p$ values increase in the same proportion as the heating rate, a property which has been widely discussed in the literature [11], and which is less evident in the case of hard-to-resolve multiple peaks.

Table 3
The activation energies and frequency factors

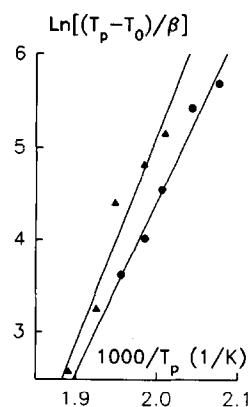| Parameter	Peak 1	Peak 2
E (kcal mol^{-1})	42.06	44.64
K_0 (s^{-1})	2.79×10^{16}	1.93×10^{17}

Fig. 3. Experimental plots and straight regression lines for both peaks of the alloy (●, peak 1; ▲, peak 2).

Bearing in mind that, in most crystallization processes, the activation energy is much larger than the product RT, the crystallization kinetics of the alloy in question was studied according to the appropriate approximation, described in the preceding theory.

Plots of $\ln[(T_p - T_0)/\beta]$ versus $1/T_p$ at each heating rate and for all stages of the process, and also the straight regression lines carried out, are shown in Fig. 3. From the slope of these experimental straight lines,
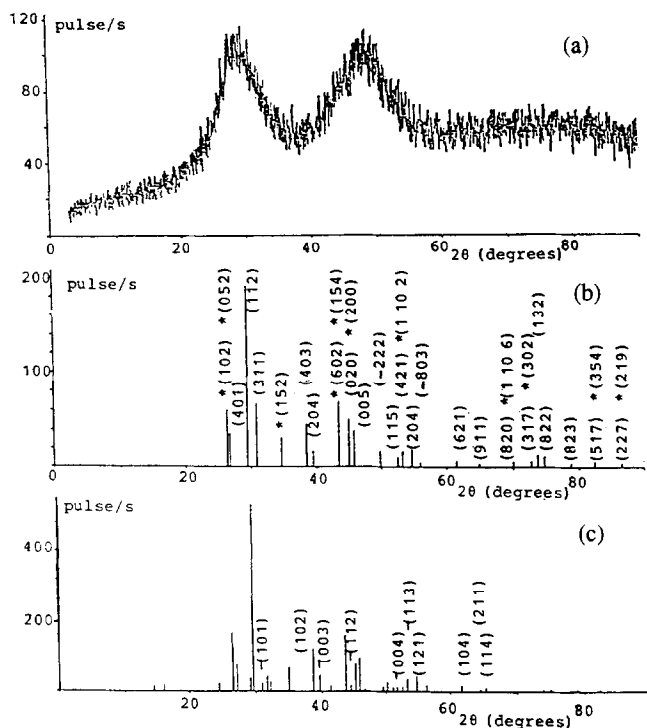
Table 4
The maximum crystallization rates, corresponding rate constants and kinetic exponents for the different heating rates

Peak	β (K min^{-1})	$10^3 (dx/dt)_p$ (s^{-1})	$10^3 K_p$ (s^{-1})	$10^3 \langle K_p \rangle$ (s^{-1})	n	$\langle n \rangle$
1	2	2.369	3.386	12.724	2.14	1.73
	4	4.003	4.652		1.73	
	8	8.471	10.295		2.08	
	16	13.513	15.861		1.88	
	32	18.667	29.424		1.06	
2	2	4.277	4.786	26.513	4.63	3.14
	4	7.249	8.498		1.87	
	8	11.174	19.039		1.72	
	16	27.295	31.857		4.07	
	32	48.687	68.385		3.39	

Fig. 4. Powder X-ray diffraction pattern for (a) as-quenched glass, (b) glass heated to the temperature T_1 and cooled (peaks marked with * correspond to Cu_7Te_5; the non-marked peaks are assigned to As_2Te_3), (c) glass heated up to complete crystallization (temperature T_2). Additional peaks appear, which are assigned to CuTe.

according to expression (10), it is possible to deduce the values of the activation energy E for the crystallization processes studied. In addition, the origin ordinate of these straight lines gives the values corresponding to the frequency factors K_0, which are given in Table 3 together with the activation energies.

By using the values of the frequency factor of the process, it is possible to calculate the value of the reaction rate constant K_p at each heating rate which corresponds to the maximum crystallization rate. The results for both magnitudes are shown in Table 4. These values make it possible to determine, through relationship (11), the reaction order n of each process corresponding to each of the experimental heating rates. This parameter is also shown in Table 4, where the rate constant corresponding to the maximum may also be observed to exhibit a similar behaviour for the crystallization rate peak values, in relation to the heating rates.

According to the Avrami theory of nucleation, the relatively high values found for the frequency factor (related to the probability of molecular collisions) seem to confirm the fact that, in the crystallization reaction mechanism, there is diffusion controlled growth, coherent with the basic formalism used.

The glassy alloy $Cu_{0.20}As_{0.35}Te_{0.45}$ shows two relatively stable crystallization stages $(E > 40 \text{ kcal mol}^{-1})$

for which the frequency factor is moderately high. The calorimetric analysis is an indirect method which only makes it possible to calculate mean values for the parameters which control the kinetics of a reaction; however, certain information can be obtained about the nucleation and crystalline growth process. According to the literature [8], the first stage shows all shapes growing from small dimensions, with a decreasing nucleation rate, whereas the second stage exhibits a crystallization mechanism with an increasing nucleation rate.

5. Identification of the crystalline phases

Taking into account the resolution of the aforementioned overlapping peaks of the glassy alloy $Cu_{0.20}As_{0.35}Te_{0.45}$, it is recommended to try to identify the possible phases that crystallize in each stage and coexist in the material after the overall crystallization by means of adequate DSC and XRD measurements. For this purpose the samples were heated at 8 K min^{-1} up to temperatures T_1 and T_2, shown in Fig. 1, and subsequently cooled to room temperature. The aforementioned temperatures were selected so as to avoid, as much as possible, interference of the second stages with the first one. The diffractograms corresponding to the samples heated at the two temperatures mentioned are shown in Fig. 4. Trace (a) of Fig. 4 has broad humps characteristic of the amorphous state of the starting material. The diffractogram of the transformed material during the first stage suggests the presence of microcrystallites of As_2Te_3 and Cu_7Te_5 (indexed in trace (b)). In the second stage, when the glassy material has already gone through the overall crystallization process, shown in Fig. 4(c), a small amount of the crystalline phase CuTe appears, coexisting with the aforementioned crystalline compounds.

The As_2Te_3 phase found crystallizes in the monoclinic system [12] with a cell unit defined by $a = 14.339$ Å, $b = 4.006$ Å, $c = 9.873$ Å and $\beta = 95°$, and the Cu_7Te_5 phase crystallizes in the orthorhombic system [13] with a cell unit defined by $a = 12.220$ Å, $b = 19.893$ Å and $c = 4.003$ Å. The CuTe crystalline phase detected in the second stage of the process shows orthorhombic symmetry [14] with the following parameters: $a = 3.16$ Å, $b = 4.08$ Å and $c = 6.93$ Å.

6. Conclusions

Crystallization of bulk $Cu_{0.20}As_{0.35}Te_{0.45}$ glass has been studied using calorimetric and X-ray powder diffraction techniques. The study of the crystallization kinetics was made using a method in which the crystallization rate is deduced bearing in mind the dependence of the reaction rate constant on time. This method for

thermal analysis of glassy alloys proved to be efficient and accurate, giving results which were in good agreement with the nature of the alloy under study, which are representative of different nucleation and crystalline-growth processes, according to the values found for the reaction order. Identification of the crystalline phases was done by recording the X-ray diffraction patterns. In the first stage of the process, microcrystallites of As_2Te_3 and Cu_7Te_5 are crystallized in an amorphous matrix. Finally, in the second transformation, the crystalline phase CuTe appears, coexisting with the aforementioned crystalline compounds.

References

[1] H.E. Kissinger, *Anal. Chem.*, 29 (1957) 1702.

[2] D.J. Sarrach and J.P. De Neufville, *J. Non-Cryst. Solids, 22* (1976) 245; D.W. Henderson, *J. Non-Cryst. Solids, 30* (1979) 301.

[3] S. Surinach, M.D. Baró, M.T. Clavaguera-Mora and N. Clavaguera, *J. Non-Cryst. Solids, 58* (1983) 209.

[4] C. Wagner, J. Vázquez, P. Villares and R. Jiménez-Garay, *J. Mater. Sci., 29* (1994) 3316.

[5] W.A. Johnson and K.F. Mehl, *Trans. Am. Inst. Mining Met. Eng., 135* (1981) 315.

[6] M. Avrami, *J. Chem Phys., 7* (1939) 1103; *8* (1940) 212.

[7] D. Turnball, *Solid State Physics*, Vol. 3, Academic Press, New York, 1956.

[8] J.W. Christian, *The Theory of Transformations in Metal and Alloys*, Pergamon, New York, 2nd edn., 1975, p. 542.

[9] J.A. Augis and J.E. Bennett, *J. Thermal Anal., 13* (1978) 283.

[10] C. Wagner, J. Vázquez, P. Villares and R. Jiménez-Garay, *Mater. Lett., 18* (1994) 280.

[11] Y.Q. Gao, W. Wang, F.Q. Zheng and X. Liu, *J. Non-Cryst. Solids, 81* (1986) 135.

[12] G.J. Carron, *Acta Crystallogr., 16* (1963) 338.

[13] T. Mizota, M. Komatsu and K. Chiara, *Mineral J., 7* (1973) 252.

[14] R.V. Baranova and Z.G. Pinsker, *Sov. Phys. Cryst., 9* (1964) 83.